JOURNAL OF WATER AND LAND DEVELOPMENT
e-ISSN 2083-4535
Polish Academy of Sciences (PAN) Institute of Technology and Life Sciences – National Research Institute (ITP – PIB)

JOURNAL OF WATER AND LAND DEVELOPMENT
DOI: 10.24425/jwld.2026.157828
2026, No. 68 (I–III): 114–120

Assessing the impact of the Yarmouk Forest Reserve fire on digital natural indices

Hashem Alshraifat*[1)], Hussam Al-Bilbisi[2)]

[1)] Ministry of Education, Khaled Bin Ahmad St, 165, 00000, Doha, Qatar

[2)] University of Jordan, Department of Geography, Queen Rania St, 45, 11942, Amman, Jordan

* Corresponding author

RECEIVED 11.04.2025 ACCEPTED 24.09.2025 AVAILABLE ONLINE 02.03.2026

Abstract: Forest fires are a major environmental hazard that threatens ecosystems and biodiversity, especially in Mediterranean regions like northern Jordan. These regions are particularly vulnerable due to their climatic characteristics, vegetation composition, and seasonal dryness, which increase the impact of forest fires. This study assesses the impact of the Yarmouk Forest Reserve fire, which occurred on May 14, 2022, using satellite-derived digital indices. The Yarmouk Forest Reserve represents an important natural ecosystem, making the assessment of fire impacts essential for environmental monitoring and management.

Landsat-8 imagery was analysed using geographic information system (GIS) tools to calculate multiple indices: the normalised difference vegetation index (*NDVI*), soil adjusted vegetation index (*SAVI*), transformed vegetation index 2 (*TVI2*), land surface temperature (*LST*), modified bare soil index (*MBI*), and normalised burn ratio index (*NBRI*). These indices are widely used to detect changes in vegetation condition, surface characteristics, and burn severity before and after fire events.

The greatest observed change was in *LST*, where the maximum temperature increased from 29.2°C to 37.5°C, indicating a clear thermal response to the fire event. Vegetation indices showed minor declines, with *NDVI* decreasing from 0.42 to 0.41, reflecting limited but detectable changes in vegetation cover. The burned area showed a noticeable increase in bare soil and burn severity, as indicated by changes in soil-related and burn-specific indices. These results underscore the need for precise, localised fire impact assessments and suggest integrating multi-temporal high-resolution data for future studies to improve the accuracy of fire impact analysis and environmental recovery monitoring.

Keywords: burned area assessment, environmental monitoring, forest fire, land surface temperature, satellite remote sensing, vegetation loss, Yarmouk Forest Reserve

INTRODUCTION

Forest fires are one of the most destructive natural hazards affecting terrestrial ecosystems. Their frequency and intensity have increased due to climate change, human activities, and land-use dynamics (Chaudhary and Piracha, 2021). These fires can range from surface-level burns to high-intensity crown fires that consume large vegetation canopies. The severity of a fire's impact depends heavily on local topography, vegetation type, and soil characteristics (Kumar and Kumar, 2020).

Causes of wildfires are generally categorised into anthropogenic and natural drivers. While human-induced factors include land clearing, agricultural burning, and negligence, natural factors such as drought, high temperatures, and lightning strikes are significant accelerators of fire spread and intensity. The ecological consequences of forest fires are far-reaching. They disrupt soil structure, reduce vegetation biomass, alter wildlife habitats, and significantly contribute to greenhouse gas emissions. Recent studies have also highlighted the socio-economic ramifications of large-scale wildfires, including health impacts, infrastructure damage, and loss of biodiversity (Bot and Borges, 2022; Rosec-Dias *et al.*, 2022).

The increasing availability of satellite remote sensing data has enabled more precise analysis of wildfire effects.

Vegetation indices such as the normalised difference vegetation index (*NDVI*), enhanced vegetation index (*EVI*), and normalised burn ratio index (*NBRI*) have become standard tools for assessing vegetation health, fire severity, and post-fire regeneration (Hartoyo *et al*., 2021; Suárez-Fernández, Martínez-Sánchez and Arias, 2025).

However, despite the global expansion of forest fire research, there remains a lack of localised studies, particularly in arid and semi-arid Mediterranean zones like Jordan. Previous work in Jordan has either focused on predictive modelling or on small-scale fire assessment (Qaralleh *et al*., 2023; Alshraifat and Al-Bilbisi, 2024). This study attempts to fill that gap by analysing multiple digital indices derived from satellite imagery to evaluate vegetation degradation following the Yarmouk Forest Reserve fire in 2022.

Therefore, this study aims to investigate the environmental consequences of the May 14, 2022, fire in the Yarmouk Forest Reserve by analysing changes in a set of vegetation-related satellite-derived indices.

The central hypothesis is that the fire caused a significant decrease in vegetation index values reflecting severe vegetation degradation and altered land surface characteristics in the affected area.

MATERIALS AND METHODS

STUDY AREA

The present study was conducted within the geographical boundaries affected by the forest fire that occurred on May 14, 2022, within the Yarmouk Forest Reserve, located in Irbid governorate in northwest Jordan. The reserve lies adjacent to the Golan Heights and covers a total area of 21 km^2, with the specific area impacted by the 2022 fire measuring approximately 1.2 km^2. The location map of the study area is illustrated in Figure 1.

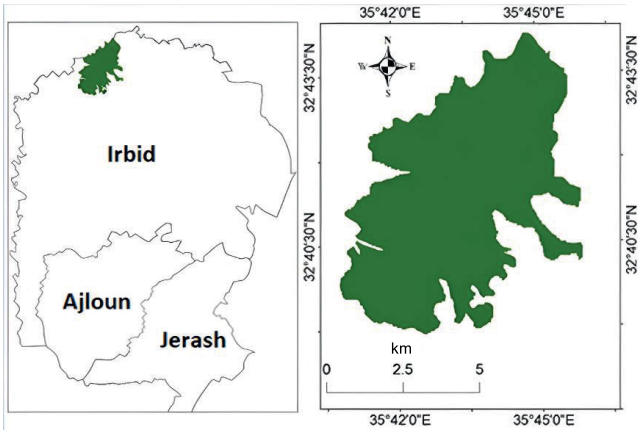

Fig. 1. Map of the study area (researchers' preparation); source: own study

The topography of the Yarmouk Forest Reserve is diverse, with altitudes ranging from 100 m below sea level in areas covered by fallen oak forests to mountainous regions reaching elevations of up to 500 m a.s.l. The climate within the reserve falls under the category of a hot Mediterranean climate, characterised by hot summers and mild, wet winters. Annual precipitation ranges from 400 to 600 mm.

The reserve hosts a rich biodiversity, comprising more than 500 plant species. Among these, the most significant in terms of ecological value are fallen-leaf oak (*Quercus* spp.), Atlantic pistachio (*Pistacia atlantica*), white willow (*Salix alba*), and eastern vegetation types. Furthermore, the reserve is home to 18 recorded mammal species, including the Arabian deer (*Gazella arabica*), jungle cat (*Felis chaus*), lynx (*Lynx* spp.), rock hyrax (*Procavia capensis*), and the golden jackal (*Canis aureus*). Avian diversity is also significant, with 127 bird species documented, in addition to 19 species of reptiles (Royal Society for the Protection of Nature, 2023).

This study employed an analytical methodology utilising satellite remote sensing data and geographic information systems, ArcMap 10.5 (Esri, USA) to assess the environmental effects of the Yarmouk Forest Reserve fire that occurred on May 14, 2022. The workflow involved several key stages, including data acquisition, image preprocessing, index calculation, and spatial analysis.

Data sources: Landsat 8 imagery from USGS (path 174, row 037), dated May 10 and May 18, 2022, with 30 m resolution. Shapefiles for boundaries were sourced from Jordan University of Science and Technology.

Processing workflow: radiometric correction, subsetting, raster calculation of six indices (normalised difference vegetation index (*NDVI*), soil adjusted vegetation index (*SAVI*), transformed vegetation index 2 (*TVI2*), land surface temperature (*LST*), modified bare soil index (*MBI*), normalised burn ratio index (*NBRI*)), and classification were conducted in ArcGIS.

Classification thresholds were adopted from published literature and adjusted to local environmental conditions.

CHANGE IN VALUES OF DIGITAL INDICES

There are numerous indices utilised to measure various benchmarks on the Earth's surface. Among these, plant indices are of paramount importance in the current field of research. A comprehensive set of indices has been developed to assess vegetation and estimate its categories and intensity. Nevertheless, other indices cannot be disregarded, as they hold significance and influence vegetation density. For instance, soil indices play a crucial role in determining vegetation density.

In arid and semi-arid regions, soil cover reflects a higher amount of near-infrared radiation (NIR) and red wavelength (RED) rays, which are commonly used as reference points in vegetation studies. Plant wavelengths are notably affected by soil components and properties, including roughness, texture, and moisture content. Additionally, soil in these areas tends to be heterogeneous, comprising a mixture of various soil types. This heterogeneity significantly contributes to the spectral reflection process (Rego, Cadima and Strand, 2020).

To evaluate the impact of environmental disturbances, such as fire, a range of indices were applied to the study area both before and after the fire. The objective was to determine the precise extent of the fire's effects on vegetation, soil moisture, and other ecological elements. Notably, two indices: the soil moisture index (*SMI*) and the atmospheric resistant vegetation index (*ARVI*) were excluded from further analysis. This decision was made because their category values remained unchanged after the fire compared to pre-fire conditions.

The formulas used for the index calculations can be found detailed in Table S1.

Normalised difference vegetation index (*NDVI*). One of the most significant indices of plant density categories is the *NDVI*. This index is derived based on the ratio between the difference in spectral reflectance at the infrared and red wavelength ranges, divided by their sum. The *NDVI* value ranges from –1 to 1, with higher values indicating a greater density of vegetation cover (Hartoyo *et al.*, 2021).

The soil-adjusted vegetation index (*SAVI*). The development of this index aims to minimise the adverse effects on soil as much as possible, particularly when extracting vegetation in areas characterised by sparse plant cover.

Transformed vegetation index 2 (*TVI2*). The development of the *TVI2* was undertaken as an enhancement of the original transformed vegetation index (*TVI*). This innovation addresses certain limitations inherent in the normalised difference vegetation index (*NDVI*), particularly its inclusion of negative values that cannot be aggregated and its lack of normal distribution. The *TVI2* accounts for the absolute values of *NDVI* categories, representing the distance between a numerical value and zero on the number line.

Land surface temperature (*LST*). Surface temperature can be derived from satellite imagery by analysing the visual data profile through a series of mathematical equations. The initial step involves calculating the radiation value above the atmosphere, which is derived from data obtained via satellite sensors. These sensors record radiation values that are influenced by various atmospheric factors, necessitating preprocessing before conducting further analysis (Tajudian *et al.*, 2021).

Modified bare soil index (*MBI*). An important index used for distinguishing bare ground from other land cover types is the *MBI*. The *MBI* employs shortwave infrared (SWIR) wavelengths and NIR data, demonstrating superior accuracy when compared to the bare soil index (*BSI*) and other similar indices. This improved accuracy significantly enhances the classification of land cover, particularly in scenarios where distinguishing bare land from urban areas is challenging due to the similarity and overlap of threshold values.

Normalised burn ratio index (*NBRI*). One of the most effective indices for assessing the proportion of fire-prone areas is the *NBRI*. This index is derived from the dependence on NIR and SWIR wavelengths, specifically utilising the 5th and 7th bands of Landsat 8 satellite imagery. The NIR band is highly sensitive to changes in chlorophyll content within vegetation, while the SWIR band aids in estimating the moisture content of both soil and vegetation.

The output values of the *NBRI* range from –1 to 1, with burned areas typically exhibiting values between 0.2 and 0.38, indicating a low proportion of burned vegetation. Values around 0.55 indicate a medium proportion of burned areas, while higher values suggest a more severe level of combustion. The *NBRI* is calculated using the following formula (Khoirunisa and Laszlo, 2020).

RESULTS

The pre- and post-fire assessment of satellite-derived indices across the Yarmouk Forest Reserve revealed varying levels of environmental change. While some indices reflected only minor shifts at the reserve scale, localised changes – especially within the 1.2 km^2 fire-affected zone – were more pronounced, particularly in surface temperature and soil exposure.

The analysis revealed that the highest normalised difference vegetation index (*NDVI*) value in the study area before the fire was 0.42, which corresponds to the medium plant density category, as presented in Table 1. In contrast, the lowest value recorded was 0. Following the fire event, the highest *NDVI* value decreased slightly to 0.41. Additionally, the area classified within the highest plant density category decreased from 13.5 km^2 before the fire to 13 km^2 after the fire, indicating a reduction of approximately 500 m^2 in the upper-density vegetation cover. This decline reflects a noticeable decrease in vegetation density. The following figure (Fig. 2) illustrates the *NDVI* maps of the study area before and after the fire, highlighting the changes in vegetation density distribution.

Table 1. Description and normalised difference vegetation index (*NDVI*) class interval for vegetation cover

Class	Classification criterion
Bare soil and/or water	$NDVI \leq 0$
Very low	$0 < NDVI \leq 0.2$
Low	$0.2 < NDVI \leq 0.4$
Moderately low	$0.4 < NDVI \leq 0.6$
Moderately high	$0.6 < NDVI \leq 0.8$
High	$0.8 < NDVI \leq 1$

Source: Aquino *et al.* (2018).

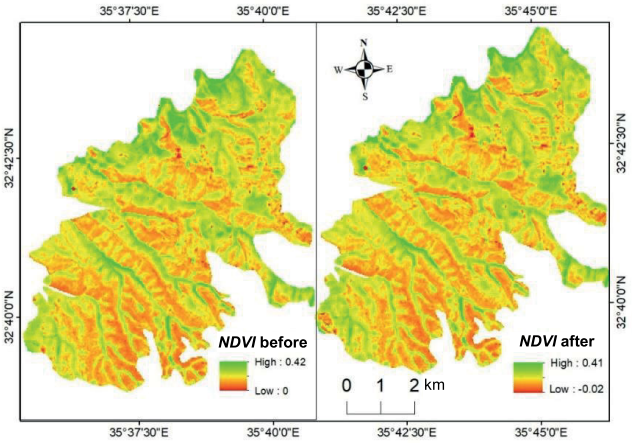

Fig. 2. Normalised difference vegetation index (*NDVI*) before and after fire; source: own study

The maximum soil adjusted vegetation index (*SAVI*) values recorded in the study area prior to the fire reached 0.63. This value corresponds to the category of low plant density, as indicated in Table 2. The total area encompassed by this category was approximately 1.59 km^2. However, after the fire, the highest value decreased to 0.62, while the minimum value declined to –0.04. The *SAVI* maps before and after the fire are presented in the following figure (Fig. 3).

The analysis revealed that the highest value of transformed vegetation index 2 (*TVI2*) within the study area prior to the fire event was 0.93. Following the fire, this value decreased slightly to

Table 2. Description and soil adjusted vegetation index (*SAVI*) class interval for vegetation cover

Vegetation density	Classification criterion of *SAVI*
No vegetation/water	<0.255
Very low	[0.255–0.450)
Low	[0.450–0.675)
Medium	[0.675–0.900]
High density	>0.900

Source: Hisham *et al.* (2022).

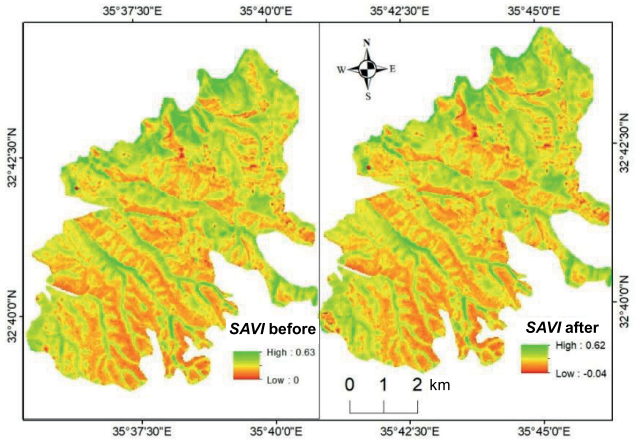

Fig. 3. Soil adjusted vegetation index (*SAVI*) before and after fire; source: own study

0.92, while the minimum index value remained consistent at 0.71. The comparative maps of the *TVI2* before and after the fire, are presented in the accompanying figure (Fig. 4).

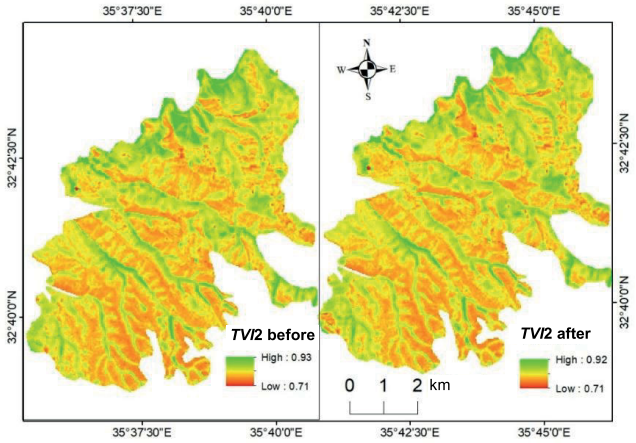

Fig. 4. Transformed vegetation index 2 (*TVI2*) before and after fire; source: own study

A discernible alteration in surface heat values between different regions of the study area was observed when comparing pre-fire and post-fire conditions. Specifically, the maximum recorded temperature increased from 29.2°C to 37.5°C, while the minimum temperature rose from 17.2°C to 24.2°C. This phenomenon can be attributed to increased surface exposure and heightened reflectivity resulting from the fire event. In the subsequent figure (Fig. 5), the land surface temperature (*LST*) maps before and after the fire are presented, illustrating these changes.

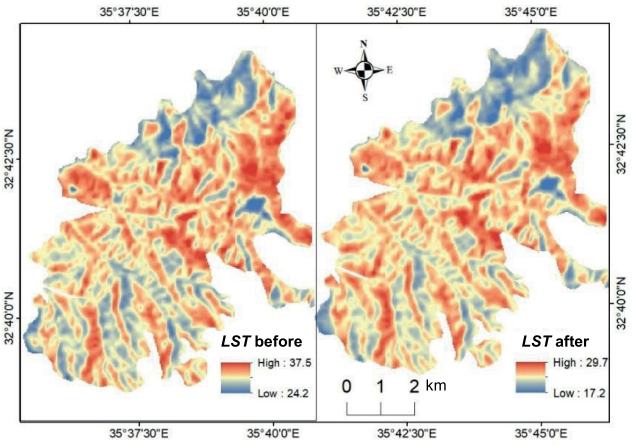

Fig. 5. Land surface temperature (*LST*) before and after fire; source: own study

With regard to the modified bare soil index (*MBI*), the analysis results revealed that the lowest pre-fire category was 0.06, while the highest value reached 0.26. In contrast, post-fire results indicated an increase, with the maximum value rising to 0.28 and the minimum value to 0.09.

The *MBI* maps of the study area, depicting the spatial distribution of bare land before and after the fire incident, are presented in the subsequent figure (Fig. 6).

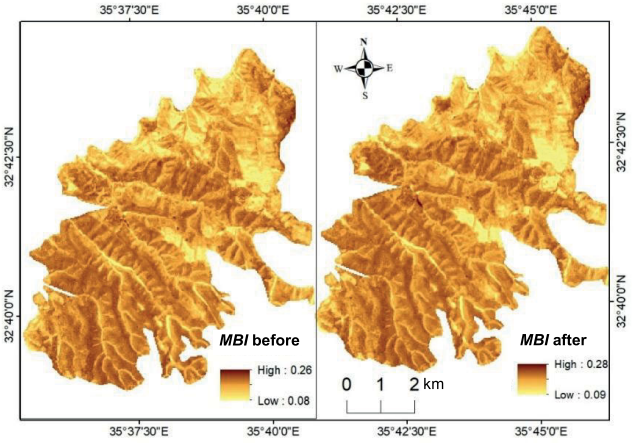

Fig. 6. Modified bare soil index (*MBI*) before and after fire; source: own study

As for the normalised burn ratio index (*NBRI*), it was found that the highest pre-fire value in the study area was 0.36, corresponding to a low proportion of burned areas. After the fire event, this value increased to 0.39, indicating a medium proportion of burned areas. The subsequent figure (Fig. 7) displays *NBRI* maps of the study area before and after the fire, highlighting the spatial distribution of burned regions.

A summary of the changes in the highest values across all assessed indices is provided in the following table (Tab. 3).

The results are summarised below, organised by index.

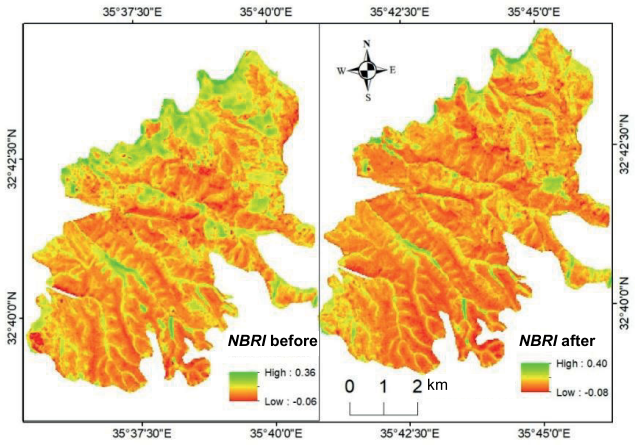

Fig. 7. Normalised burn ratio index (*NBRI*) before and after fire; source: own study

Table 3. The highest values of all indices before and after fire

Index	The highest value before fire	The highest value after fire
NDVI	0.42	0.41
SAVI	0.63	0.62
TVI2	0.93	0.92
LST	29.7	37.5
MBI	0.26	0.28
NBRI	0.36	0.39

Explanations: *NDVI* = normalised difference vegetation index, *SAVI* = soil adjusted vegetation index, *TVI2* = transformed vegetation index 2, *LST* = land surface temperature, *MBI* = modified bare soil index, *NBRI* = normalised burn ratio index.
Source: own study.

Normalised difference vegetation index. The values of *NDVI* in the study area exhibited a slight decline following the fire event. The maximum *NDVI* value decreased from 0.42 (pre-fire) to 0.41 (post-fire), indicating a modest reduction in overall vegetation greenness. However, spatial analysis revealed a more meaningful ecological change: areas with dense vegetation (*NDVI* > 0.4) shrank by approximately 0.5 km^2. This reduction suggests that while the overall average *NDVI* may not have changed significantly, localised vegetation loss did occur within the fire perimeter. The visual comparison of pre- and post-fire *NDVI* maps (Fig. 2) clearly shows patches of vegetative degradation concentrated in the southern part of the affected zone.

Soil-adjusted vegetation index. The *SAVI* remained relatively stable, with a slight decrease from a maximum of 0.63 before the fire to 0.62 afterwards. However, the minimum *SAVI* value dropped from near zero to –0.04, indicating localised vegetation stress or removal, particularly in areas with sparse cover and high soil reflectance. While the average change was minimal at the reserve scale, a closer inspection of *SAVI* distribution maps (Fig. 3) suggests reduced vegetation health in areas directly impacted by fire, particularly in topographically exposed or sloped regions.

Transformed vegetation index 2. The *TVI2* values marginally declined from 0.93 to 0.92. Although this decrease is numerically insignificant, it signals a small reduction in the photosynthetic activity of vegetation. Since *TVI2* is designed to mitigate the statistical limitations of *NDVI* (e.g., negative values and non-normal distributions), its consistent performance across the landscape reinforces the detection of subtle post-fire vegetation stress. Spatially, the most significant drops in *TVI2* correspond with known burn areas (Fig. 4).

Land surface temperature. Among all the analysed indices, *LST* exhibited the most dramatic change. The maximum surface temperature increased sharply from 29.2°C (pre-fire) to 37.5°C (post-fire), and the minimum temperature rose from 17.2°C to 24.2°C. This 8.3°C increase in maximum *LST* reflects a significant shift in surface energy dynamics due to vegetation loss, increased albedo, and soil exposure. The thermal maps (Fig. 5) reveal distinct heat islands corresponding to the fire perimeter, suggesting a major alteration in the microclimatic conditions of the area.

Modified bare soil index. The *MBI* increased from 0.26 to 0.28, indicating a greater presence of bare or sparsely vegetated soil surfaces after the fire. Since the *MBI* incorporates *SWIR* and *NIR* reflectance to distinguish bare ground from vegetated or urban surfaces, the observed increase reflects fire-induced vegetation removal and subsequent soil exposure. Post-fire *MBI* maps (Fig. 6) show a concentration of higher values in previously vegetated areas, especially near the centre of the burned zone.

Normalised burn ratio index. The *NBRI* values rose from 0.36 before the fire to 0.39 afterwards. This moderate increase transitions the area's classification from low to medium burn severity, according to thresholds established in prior studies. The *NBRI* was particularly sensitive to burned vegetation in areas where *NDVI* and *SAVI* changes were subtle, making it a reliable indicator of combustion effects (Fig. 7). This result aligns with field reports that the fire was moderately intense and localised (Tab. 4).

Table 4. Summary of index value changes

Index	Pre-fire max	Post-fire max	Observed change
NDVI	0.42	0.41	slight decrease; 0.5 km^2 vegetation loss
SAVI	0.63	0.62	slight decrease; minimum dropped to –0.04
TVI2	0.93	0.92	marginal decline; stable minimum
LST	29.2	37.5	substantial increase of 8.3°C
MBI	0.26	0.28	increased bare soil reflectance
NBRI	0.36	0.39	indicates medium burn severity

Explanations: *NDVI*, *SAVI*, *TVI2*, *LST*, *MBI*, *NBRI* as in Tab. 3.
Source: own study.

Spatial perspective: burned vs unburned zones. When focusing only on the 1.2 km^2 burned area, all indices showed more pronounced changes compared to the entire 21 km^2 reserve. The *NDVI* and *SAVI* exhibited greater reductions locally, while *LST* and *MBI* values sharply increased. This contrast highlights the challenge of interpreting averaged index values over large areas that include unburned zones. It also reinforces the importance of subsetting and spatial masking in future studies to isolate the fire's true ecological impact.

DISCUSSIONS

The results of this study demonstrate the efficacy of satellite-derived indices in detecting and quantifying environmental changes following forest fires. While the vegetation indices (normalised difference vegetation index (*NDVI*), soil adjusted vegetation index (*SAVI*), and transformed vegetation index 2 (*TVI2*)) showed only marginal reductions at the scale of the entire Yarmouk Forest Reserve, localised impacts within the fire perimeter were more distinct – especially in indices that capture thermal and soil exposure characteristics.

Verification and validation methods have been used during the study. To ensure the validity of the findings, a multi-method verification approach was adopted.

1. **Comparative analysis with previous studies**. The observed changes in *NDVI* and *SAVI* were compared with regional and global post-fire studies. For instance, Qaralleh *et al*. (2023) and Al-Zubaidi (2023) reported slightly greater reductions in *NDVI* (typically between 0.03 and 0.08) in burned areas of northern Jordan. However, those studies focused exclusively on fire-affected zones, whereas this study included the entire reserve. When adjusting for scale, our observed change in *NDVI* (–0.01) is consistent with expected reductions in similar Mediterranean environments after moderate fires (Bot and Borges, 2022; Suárez-Fernández, Martínez-Sánchez and Arias, 2025).
2. **Internal cross-index consistency.** An essential form of internal validation involved assessing whether changes in different indices support one another. The increase in the modified bare soil index (*MBI*) and land surface temperature (*LST*), for example, is logically coherent with the decline in vegetation indices. This reinforces the credibility of the remote sensing workflow and confirms that the fire led to both vegetation loss and increased surface exposure.
3. **Statistical change threshold interpretation.** While this study did not employ traditional inferential statistical tests (e.g., *T*-tests or ANOVA) due to the categorical nature of the indices and the raster data structure, it applied classification thresholds based on well-established literature (Aquino *et al*., 2018; Khoirunisa and Laszlo, 2020). These thresholds allowed for meaningful interpretation of changes beyond random noise or sensor variation. Furthermore, the spatial distribution of changes was not random but strongly concentrated within the known fire perimeter, providing additional evidence for the fire's localised ecological impact.
4. **Temporal consistency and control window.** To minimise confounding factors such as seasonal variation, satellite imagery was selected from dates only eight days apart (May 10 and May 18, 2022), both within the same phenological phase. This temporal control supports the attribution of changes to the fire event rather than unrelated climatic or phenological factors.

The behaviour of the indices can be interpreted as follows.

- The slight decline in *NDVI* and *SAVI* can be attributed to the averaging effect over the full 21 km^2 of the reserve, of which only 1.2 km^2 was affected by the fire. These indices are sensitive to chlorophyll content but less responsive in mixed-pixel environments.
- In contrast, *LST* displayed a substantial increase, from 29.2°C to 37.5°C. This result is consistent with post-fire studies (e.g., Lemenkova and Debeir, 2023), where loss of vegetative shading and exposure of dry soil leads to significantly higher surface temperatures.
- The rise in *MBI* indicates a measurable increase in bare land exposure, consistent with both visual interpretation of imagery and burn severity indicators.
- The values of *NBRI* increased moderately from 0.36 to 0.39, marking a shift from low to medium burn severity. According to Khoirunisa and Laszlo (2020), such values correspond to partial combustion – a finding in agreement with local field reports and ecological observations.

Limitations and recommendations for further validation. The primary limitation of this study is the spatial averaging over the entire reserve, which likely underestimates fire impact in the burned area. In future work, the analysis should employ zonal statistics confined strictly to the burn scar for more accurate quantification.

Additionally, the use of ground truth data (e.g., field surveys or drone imagery) would allow for quantitative accuracy assessment (e.g., error matrices or kappa statistics), which was not possible in the current study due to access limitations.

CONCLUSIONS

This study demonstrates that satellite-derived indices can effectively quantify the impact of forest fires on vegetation cover, surface temperature, and soil exposure within the Yarmouk Forest Reserve. Although vegetation indices (normalised difference vegetation index (*NDVI*), soil adjusted vegetation index (*SAVI*), transformed vegetation index 2 (*TVI2*)) showed only slight declines when analysing the entire reserve, marked increases in land surface temperature (*LST*) and modified bare soil index (*MBI*) reveal significant fire-induced disturbances.

Recommendations:

1) focus future analyses on precise burn perimeters rather than the entire reserve to enhance the detection of fire effects;
2) utilise multi-temporal imagery across different seasons to monitor vegetation recovery and long-term ecological changes;
3) integrate multiple indices – including thermal, vegetation, and soil-related measures – to provide a holistic assessment;
4) employ higher spatial resolution data (e.g., Sentinel-2) to capture subtle changes in the fire-affected areas;
5) combine remote sensing data with local ecological and soil information to improve result interpretation;
6) leverage these findings to inform fire risk mapping and guide targeted ecological restoration initiatives;
7) encourage cross-regional comparisons to validate remote sensing methodologies in diverse ecological contexts.

SUPPLEMENTARY MATERIAL

Supplementary material to this article can be found online at: https://www.jwld.pl/files/Supplementary_material_68_Alshraifat.pdf.

CONFLICT OF INTERESTS

All authors declare that they have no conflict of interests.

REFERENCES

Alshraifat, H. and Al-Bilbisi, H. (2024) "Forest fire prediction in northwest Jordan," *An-Najah University Journal for Research – B (Humanities)*, 38(6), pp. 1121–1154. https://doi.org/10.35552/0247.38.6.2215. [In Arabic].

Al-Zubaidi, H. (2023) "Risk of forest fires in southwest Saudi Arabia using remote sensing and geographic information systems: Shaf Shahran as a model," *Arab Journal of Geographic Information Systems*, 16(2), pp. 1–39. Available at: https://sgs.ksu.edu.sa/ar/node/3842 (Accessed: February 12, 2025). [In Arabic].

Aquino, D. *et al.* (2018) "Use of remote sensing to identify areas at risk of degradation in the semi-arid region," *Revista Ciência Agronômica*, 49(3), pp. 420–429.

Bot, K. and Borges, J. (2022) "A systematic review of applications of machine learning techniques for wildfire management decision support," *Inventions*, 7(15), pp. 1–30. Available at: https://doi.org/10.3390/inventions7010015.

Chaudhary, M. and Piracha, A. (2021) "Natural disasters – Origins, impacts, management," *Encyclopedia*, 1(4), pp. 1101–1131. Available at: http://doi.org/10.3390/encyclopedia1040084.

Hartoyo, A. *et al.* (2021) "Normalized difference vegetation index (NDVI) analysis for vegetation cover in Leuser Ecosystem area, Sumatra, Indonesia," *Biodiversitas*, 22(3), pp. 1160–1171. Available at: https://doi.org/10.13057/biodiv/d220311.

Hisham, N. *et al.* (2022) "Monitoring of rice growth phases using multi-temporal Sentinel-2 satellite image," *IOP Conference Series: Earth and Environmental Science*, 1051, 012021. Available at: https://doi.org/10.1088/1755-1315/1051/1/012021.

Khoirunisa, R. and Laszlo, M. (2020) "Burned region analysis using normalized burn ratio index (NBRI) in 2019 forest fires in Indonesia (Case study: Pinggir-Mandau District, Bengkalis, Riau)," *Geographica: Science and Education Journal*, 2(1), pp. 1–9. Available at: https://doi.org/10.31327/gsej.v2i1.1293.

Kumar, S. and Kumar, S.H. (2020) "Forest fires: Causes and impact on environment," *Just Agriculture*, 1(2), pp. 53–55.

Lemenkova, P. and Debeir, O. (2023) "Computing vegetation indices from satellite images using GRASS GIS scripts for monitoring mangrove forests in the Coastal Landscapes of Niger Delta, Nigeria," *Journal of Marine Science and Engineering*, 11(4), 871. Available at: https://doi.org/10.3390/jmse11040871.

Nguyen, C. *et al.* (2021) "A modified bare soil index to identify bare land features during agricultural fallow-period in Southeast Asia using Landsat," *Land*, 10(3), 231. Available at: https://doi.org/10.3390/land10030231.

Qaralleh, B. *et al.* (2023) "Assessment of small-extent forest fires in semi-arid environment in Jordan using Sentinel-2 and Landsat sensors data," *Forests*, 14(1), 41. Available at: https://doi.org/10.3390/f14010041.

Rego, F., Cadima, I. and Strand, E. (2020) "A log-ratio vegetation index (LRVI) for discrimination and classification of remote sensing data," *Silva Lusitana*, 28(1), pp. 45–70. Available at: https://doi.org/10.1051/silu/20202801045.

Rosec-Dias, J. *et al.* (2022) "A global synthesis of fire effects on ecosystem services of forests and woodlands," *Frontiers in Ecology and the Environment*, 20(3), pp. 170–178. Available at: https://doi.org/10.1002/fee.2349.

Royal Society for the Protection of Nature (2023) *Annual report.* Available at: https://www.rscn.org.jo/anuual-report (Accessed: February 12, 2025). [In Arabic].

Solymosi, K., Kövér, G. and Romvári, R. (2019) "The development of vegetation indices: A short overview," *Acta Agraria Kaposváriensis*, 23(1), pp. 75–90. Available at: https://doi.org/10.31914/aak.2264.

Suárez-Fernández, G., Martínez-Sánchez, J. and Arias, P. (2025) "Assessment of vegetation indices for mapping burned areas using a deep learning method and a comprehensive forest fire dataset," *Advances in Space Research*, 75(2), pp. 1665–1689. Available at: https://doi.org/10.1016/j.asr.2024.12.001.

Tajudian, N. *et al.* (2021) "Soil moisture index estimation from Landsat 8 images for prediction and monitoring landslide occurrences in Ulu Kelang, Selangor, Malaysia," *International Journal of Electrical and Computer Engineering*, 11(3), pp. 2101–2108. Available at: http://doi.org/10.11591/ijece.v11i3.pp2101-2108.